



Nanoindentation Characteristics of Stem Cells Towards Osteogenic Differentiation in a Nanoscale Vibratory Bioreactor

Reza Ramezani Sarbandi¹ · Mohammad-Mehdi Khani^{2,3} · Kamran Hassani¹ · Mohammad Tafazzoli-Shadpour⁴ · Abdolreza Ardeshiryajimi² · Mohammad Tabatabaei⁴

Accepted: 15 July 2024

© The Author(s), under exclusive licence to Springer Science+Business Media, LLC, part of Springer Nature 2024

Abstract

Mimicking chemical and physical cues present in the microenvironment of the original tissue not only facilitates the differentiation process of mesenchymal stem cells but also contributes to the attainment of cells with morphology and functionality closely resembling those of the native tissue. Among the types of mechanical stimuli utilized to induce osteogenic differentiation of stem cells, nanoscale vibrations were the focus of the present study. By investigating osteoblast-specific proteins following 21-day exposure to nanovibrational stimuli, our research confirms previous findings that highlight the upregulation of specific osteogenic proteins, including osteocalcin, osteopontin, and collagen type I. Here, we addressed the lack of investigation into the mechanical properties of mesenchymal stem cells subjected to nanovibration stimulation as a cellular differentiation biomarker. From a mechanical perspective, our findings revealed a remarkable elevation in Young's modulus, which increased by approximately 100% over the nucleus, coupled with a notable 60% reduction in the viscosity of differentiated mesenchymal stem cells after 21 days of continuous 1-kHz nanovibrational stimulation. Such alterations are associated with thicker and more aligned actin bundles, indicating a robust cellular response to mechanical stimuli. Our results can be beneficial for cell-based regenerative therapy when stem cells are intended to be manipulated in vitro before transplantation.

Keywords Nanoscale vibration · Cell mechanics · Mechanobiology · Nanoindentation · Cytoskeletal development

Highlights

- Nanovibrational stimuli differentiate HUC-MSCs into osteogenic cells
- Mechanical properties of HUC-MSCs alter in response to nanoscale vibration
- Subjection to nanoscale vibration leads to thicker and more aligned actin bundles in HUC-MSCs
- Exposure to nanoscale vibration increases Young's modulus in both the nucleus and cytoplasm area of HUC-MSCs
- Notable reductions in the viscosity of HUC-MSCs are observed due to nanovibrational stimuli

✉ Mohammad-Mehdi Khani
Khani@sbmu.ac.ir

¹ Department of Biomedical Engineering, Science and Research Branch, Islamic Azad University, Tehran, Iran

² Medical Nanotechnology and Tissue Engineering Research Center, Shahid Beheshti University of Medical Sciences, Tehran, Iran

³ Department of Tissue Engineering and Applied Cell Sciences, School of Advanced Technologies in Medicine, Shahid Beheshti University of Medical Sciences, Tehran, Iran

⁴ Department of Biomedical Engineering, Amirkabir University of Technology, Tehran, Iran

1 Introduction

Cellular differentiation, transitioning from embryonic stem cells to specialized cells in specific tissues, is influenced by the conditions of the local microenvironment. Essentially, external biological, chemical, and physical cues originating from the microenvironment play vital roles in determining cell fate [1, 2]. Cells perceive and respond to these external cues through their receptors, triggering signaling cascades that ultimately transmit signals to the nucleus [3]. Recent advancements in tissue engineering have emphasized the importance of controlling the environmental conditions within bioreactors to achieve the highest degree of resemblance to native tissue in terms of appearance and functional characteristics [4, 5].

Although biochemical signals exert a significant influence on cell fate during differentiation, the passive mechanical properties of the extracellular matrix, such as porosity, roughness, and elastic modulus, as well as the active mechanical properties, such as a complex series of forces exerted on cells, are critical determinants of cellular

outcomes. It has been highlighted that mechanical stimuli, both at the macro- and microscale, regulate various behaviors of mesenchymal stem cells [2].

a series of diverse physical cues that contribute to tissue remodeling and function. Therefore, several studies have shown the crucial role of mechanical stimuli in bone tissue formation [6, 7], and this has been proposed as an effective strategy for mimicking cartilage, ligament, and bone engineering [8, 9]. Recently, there has been growing interest in the impact of nanoscale mechanical cues on cell fate and differentiation. Studies have revealed that exerting mechanical stimuli through structural alterations in the microenvironment of the cell may lead to the induction of various differentiations. Notably, Previous studies have shown that cells may react to nanoscale cues, particularly nanotopography, by modifying gene expression and cell functions such as migration and adhesion potential [9, 10].

It is well described that nanovibration stimuli have a much more pronounced impact on inducing osteogenesis than other passive cues such as rigidity and stiffness [11, 12]. It has been shown that 14-day nanovibration stimuli promote the growth and proliferation of MSCs [13]. This suggests that vibration stimulation provides active conditions akin to the *in vivo* microenvironment, which may promote differentiation. Recently, it has been stated that low-magnitude high-frequency vibration (LMHFV) plays a crucial role in cartilage and bone engineering. LMHF loading boosted chondrogenic differentiation through alteration in the β -catenin signaling pathway [14]. Similarly, LMHF vibration enhances the expression of osteoblastic genes and proteins involved in bone formation and remodeling [8]. Low-magnitude mechanical vibration facilitates osteogenic differentiation of periodontal ligament stem cells (PLSC) through elevation of ALP, OCN, Col-I, Runx2, and OSX expression. Conversely, higher magnitude vibration directs PLSCs towards tendogenic differentiation by elevation in Col I and Col III and reduction in SOX9, PPAR- γ [15], and scleraxis level of expression [16]. It was also revealed that the amplitude of nanovibration has a direct impact on gene expression [15]. In addition, changes in the frequency of nanoscale loading significantly altered osteogenesis biomarkers, with mesenchymal stem cells expressing higher levels of bone morphogenic protein 2 (BMP2), RUNX2, and osteocalcin in response to 1-kHz stimulation compared to 500 Hz [17].

In addition to the upregulation of specific biomarkers, nanovibration alters the arrangement of cytoskeletal elements. External vibration cues increase the diameter of actin bundles [16], leading to a more organized actin fiber structure, increased cell spreading, and larger focal adhesions [17]. Although previous studies have investigated the impact of

Based on their function, each tissue type endures a different set of physical stimuli that can be directly or indirectly transmitted to the nucleus. For instance, bone tissue faces

nanovibrational stimulation on the osteogenic differentiation of stem cells in 2D and 3D cell culture [11, 18], alterations in the elastic and viscoelastic properties of stem cells in response to nanovibration have not been studied. Cell mechanical behavior is strongly correlated with cytoskeletal development, capability for traction force generation, deformability, and resilience to diverse external cues [17]. In cell-based therapy, it is necessary that stem cells have proper mechanical and structural properties to withstand the physiological load in the host tissue [19]. Therefore, a more profound correlation between the mechanical properties of stem cells and cell differentiation assists in controlling the differentiation process and helps us effectively use external cues to achieve functional cells in cell-based therapy and tissue engineering strategies [20, 21].

In the present study, we utilized a custom-made nanovibrational bioreactor to induce the osteogenic differentiation of HUC-MSCs. We then employed atomic force microscopy (AFM) to evaluate the nanoindentation characteristics of stem cells, as well as to monitor the alteration in actin filament organization during differentiation.

2 Methods and Materials

2.1 Cell Culture

Human umbilical cord-derived mesenchymal stem cells (HUC-MSCs), isolated from a donated umbilical cord tissue sample, were acquired from SinaCell Research and Production Co. (Iran, Tehran) and kept in 5% CO₂ and 95% humidity conditions at 37 °C inside an incubator. The stem cells were maintained in a T-75 cell culture flask (SPL, Korea) containing Dulbecco's Modified Eagle Medium (Thermo Fisher Scientific, USA) supplemented with 10% fetal bovine serum (FBS) (Gibco, USA), 1% penicillin/streptomycin (Sigma-Aldrich, USA), and 2 mM L-Glutamine (Sigma-Aldrich, USA). Upon reaching 80–90% confluency, cells were passaged and subcultured with 1:2 ratios. All experiments and cryopreservation were conducted in passages 3 to 7 of HUC-MSCs. Four different groups consisting of control and days 7, 14, and 21 were introduced, and the control group was cultured in a similar condition to other groups, while it was not exposed to nanovibration stimuli. Notably, the data presented for the control group are the average results of the evaluation of mesenchymal stem cells over different culture times for up to 10 days before cell passage.

2.2 Bioreactor Preparation

In the present study, a fully mechanical bioreactor was employed to apply continuous nanoscale vibrations with specific amplitudes and frequencies to HUC-MSCs, which was previously described in detail [15]. As depicted in Fig. 1, the general configuration of the bioreactor consists of a substantial 2-mm-thick glass plate serving as both a vibration absorber and a base for the system, a P-885.11 piezoelectric function as a vibration stimulator, a petri dish holder, and a petri dish as a suitable container for the cultivation of mesenchymal stem cells. Utilizing a thick glass plate minimizes energy dissipation and ensures the efficient transmission of vibrational loading in the desired direction. Each piezoelectric was directly affixed to the bottom of a 3.5-cm Petri dish containing HUC-MSCs. A thin layer of super glue was applied to ensure strong adhesion between the upper surface of the piezoelectric material and the bottom of the petri dish, thereby reducing the dissipated vibration. The frequency and amplitude of the piezoelectric were controlled and monitored using an electrical source (Pintek, FG-52) and digital oscilloscope (Instek, G05-620), respectively. Before initiating the experiments, a laser vibrometer was used to calibrate the piezoelectric range of motion, and displacements between 30 and 80 nm were measured at a frequency of 1 kHz, as reported in our previous study [15].

To provide similar experimental conditions, all the control and treated groups were placed at equal distances from each other on a thick glass plate. The bioreactor generated continuous vibration loading for 7, 14, and 21 days in 3.5-cm Petri dishes containing HUC-MSCs. This arrangement ensured that all piezoelectrics received an equivalent electrical current and that all Petri dishes were subjected to identical conditions, creating a uniform environment for the cultured cells in each dish.

The materials used in the bioreactor structure were maintained under high-humidity conditions. As a result, the entire system structure, except for the electrical source and digital oscilloscope, was placed inside the incubator at 37 °C, 5% CO₂, and 95% humidity.

2.3 Measurements of Mechanical Properties with Nanoindentation Test

Utilizing the atomic force microscope (AFM) provides the potential to perform localized evaluation of the mechanical properties of the cells. Through this, we were able to monitor the alteration in elastic and viscoelastic properties of two distinct areas (nucleus and cytoplasm) of human umbilical cord-derived mesenchymal stem cells after prolonged exposure to nanovibration stimuli. To do so, we employed a JPK microscope (Nanowizard 3) using a quadratic cantilever (K , 0.2 N/m) to measure force–displacement (elastic) and force–time (viscoelastic) relationship for control and stimulated groups. Prior to commencing the experiments, the sensitivity and actual spring constant of the cantilever were measured by performing a force–distance curve on a rigid substrate and thermal noise measurement, respectively.

To evaluate elastic property (Young's modulus), a specific region of $1\ \mu\text{m} \times 1\ \mu\text{m}$ was selected either over the nucleus or cytoplasm of desired cells. The area was divided into 64 points, equidistant from each other. The cantilever tip was approached above the first point, and it automatically indented all 64 points to a depth of 0.5 μm , at the rate of 2 $\mu\text{m/s}$ (Fig. 2A). Through that, the indentation depth was kept smaller than 10% of the cell height to ensure minimal substrate effects [22].

JPKSPM Data Processing software was used to derive elastic properties of the nucleus and cytoplasm areas of the cells. To evaluate Young's modulus, force–displacement data of the extend section were selected, and the Hertz-Snoden

Fig. 1 Schematic of nanoscale vibratory system and connection between different components

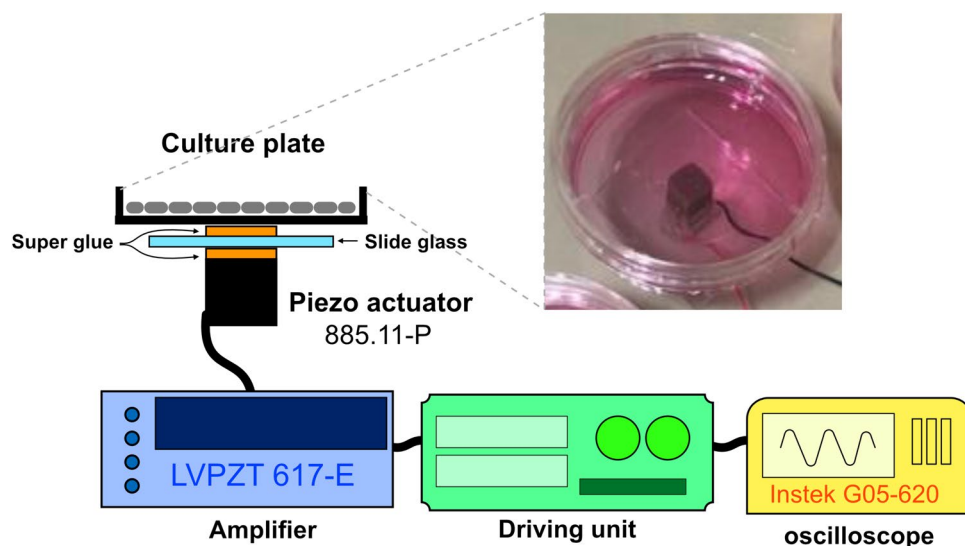
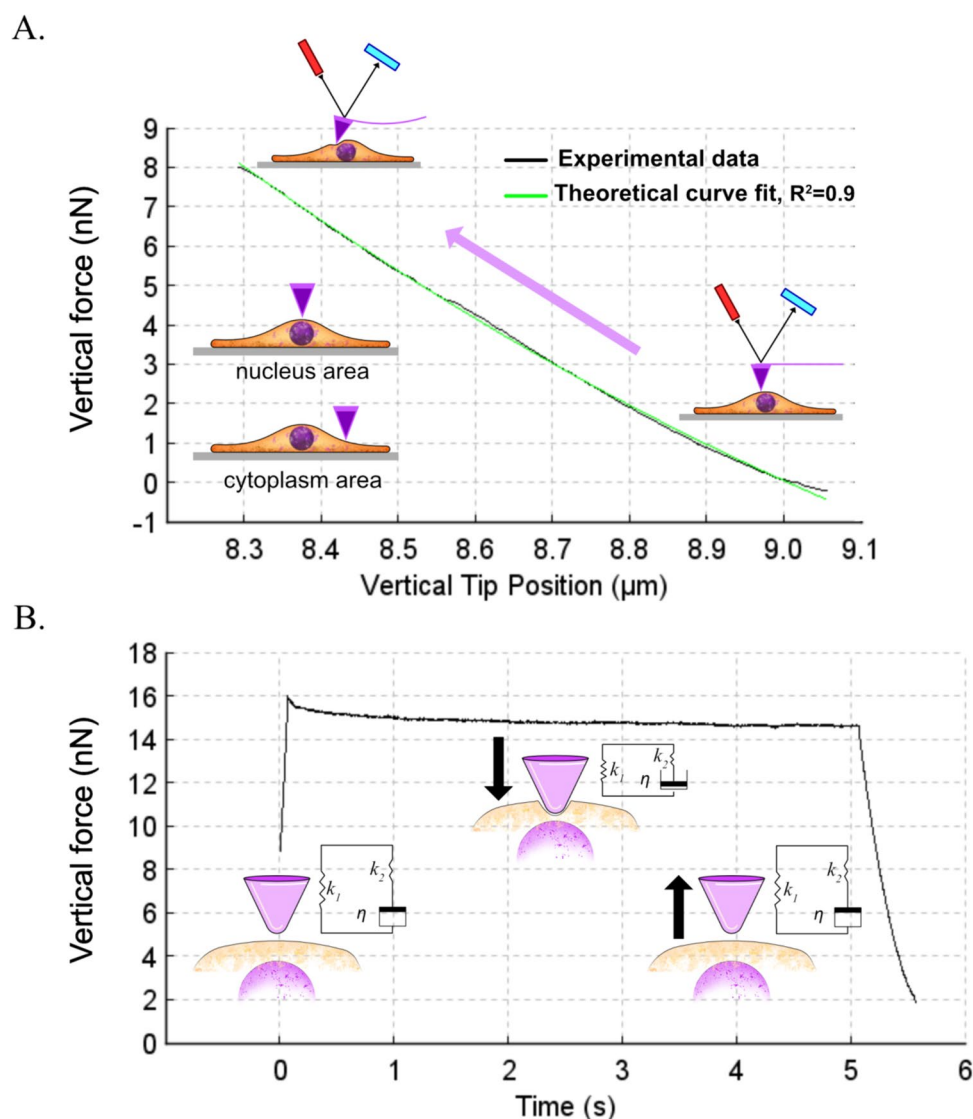


Fig. 2 A representative illustration of the results obtained from the elastic and viscoelastic experiments, **A** a typical experimental evaluation of the elastic curve by use of the AFM method in both nucleus and cytoplasm areas of HUC-MSCs. **B** A typical force–time curve used to measure viscoelastic parameters using the SLS model



model was utilized to calculate elastic property using the following equation:

$$F = \frac{E(\tan\alpha)\Delta^2}{\sqrt{2}(1-\nu^2)} \quad (1)$$

where “ α ,” “ F ,” and “ E ” stand for the opening angle of the tip, applied force, and Young’s modulus, respectively. Assuming the incompressibility of cells, Poisson’s ratio value of 0.5 was selected.

In a manner similar to the experiments conducted for elastic properties, the viscoelastic behavior of the region above the nucleus was evaluated. Stress-relaxation test was employed to assess the viscoelastic properties of the cells. The approach mechanism of the cantilever was adjusted to approach the designated area, indent to a depth of 0.5 μm at

a rate of 2 $\mu\text{m/s}$, hold the position for 5 s, and then retract about 0.5 μm (Fig. 2B).

To describe the exponential decay of heterogeneous materials, a generalized standard-linear-solid model with arbitrary Maxwell arms arranged in parallel is utilized [23]. The time-dependent relaxation modulus, $E_{\text{rel}}(t)$, is expressed by the following equation:

$$E_{\text{rel}}(xt) = E_0 + \sum_{i=1}^N E_i \exp\left(-\frac{t}{\tau_i}\right) \text{ where } \tau_i = \frac{\eta_i}{E_i} \quad (2)$$

where t is the time, E_i ($i=0, 1, \dots$) represents the elastic modulus of the i -th spring. τ_i and η_i ($i=1, 2, \dots$) are the relaxation time and apparent viscosity of the i -th dashpot, respectively. The sum of the elastic moduli, $\sum E_i = E_0 + E_1 + \dots$ accounts for the instantaneous elastic response.

The viscoelastic parameters were obtained by incorporating the transient function of Eq. (2) into the Hertz model in Eq. (1), resulting in the relaxation response given by [24, 25]:

$$F = \frac{\tan\alpha\delta^2}{\sqrt{2}(1-\vartheta^2)} \left[E_0 + \sum_{i=1}^N E_i \exp\left(-\frac{t}{\tau_i}\right) \right] \quad (3)$$

In the present study, the basic configurations of standard-linear-solid (SLS) were chosen, resulting in the following equation:

$$F = \frac{\tan\alpha\delta^2}{\sqrt{2}(1-\vartheta^2)} \left[E_1 + E_2 \exp\left(-\frac{t}{\tau}\right) \right] \quad (4)$$

where E_1 and E_2 are the instantaneous and equilibrium moduli, respectively. The relationship between the instantaneous and equilibrium moduli with a constant spring in the SLS model (Fig. 2B) is as follows [20, 26]:

$$E_1 = \frac{3}{2}(k_1 + k_2) \quad (5)$$

$$E_2 = \frac{3}{2}k_1 \quad (6)$$

All computations and fittings were performed by developing a customized subroutine in Matlab R2021a (Mathworks Inc., Natick). A schematic presentation of force–displacement (elastic) and force–time (viscoelastic) curves obtained is demonstrated in Fig. 2.

During the analysis of AFM data, some data were excluded from the analysis. Owing to the different parameters, such as the correct amount of indentation considering the total cellular height and structural conditions within the cell, some data may not be suitable for further evaluation. In this case, the hard substrate of the cell may affect the ultimate force–distance relationship. In such cases, the local slope of the force–distance curves changed drastically, indicating that the AFM tip was very close to the substrate, thereby overestimating the detected force. In addition, the curve containing the turbulence caused mainly by external noise was excluded.

2.4 Cytoskeleton Staining

Following continuous exposure to mechanical loading for some specific durations (7, 14, or 21 days), actin fibers were visualized using a fluorescent microscope prior to immunostaining. First, the cells were fixed using a 4% paraformaldehyde solution after removal of the culture medium. Next, the membranes of the sample cells were permeabilized by exposing the cells to a 0.1% Triton X-100 solution for 15 min. The

triton solution was then removed, and the cells were washed twice with PBS. To prevent non-specific binding, 1% BSA was added to the Petri dish, followed by washing twice with PBS.

To stain the desired proteins, the cells were incubated overnight at 4 °C with an anti-vinculin primary antibody (FAK100, Sigma-Aldrich). Next, the primary antibody solution was removed, and the cells were washed with PBS before being exposed to a solution containing a fluorescent-labeled secondary antibody and Alexa Fluor 488 Phalloidin for 1 h. The samples were washed three times with PBS and then exposed to DAPI solution to stain the nuclei. Finally, a fluorescent microscope (Olympus, IX71, USA) was used to visualize vinculin, actin fibers, and nuclei.

To quantify actin filament organization, we defined three parameters: number of actin bundles, actin bundle diameters, and their relative orientations. Image processing software (ImageJ) was employed to enhance the quality of the images, enabling better distinction between the actin bundles and background. Utilizing the proper tools of ImageJ software, we measured both the number and diameter of actin bundles in numerous cells for the control and stimulated groups. To measure the diameter and number of actin fibers, a line perpendicular to the fiber was drawn, and the diameter of the fibers and their quantity per cell were calculated based on the color intensity of different locations. In addition, to quantify the actin bundle alignment, a reference line was chosen, and the angle between each actin bundle and the reference line was measured.

2.5 Immunohistochemistry

To prepare samples for immunohistochemistry analysis, cells were isolated from sample Petri dishes connected to piezoelectrics using trypsin solution. The culture medium inside the Petri dish was removed, and trypsin solution was added. The suspended cells were then transferred to sterile tubes for centrifugation. The cells were then resuspended in 1 ml of 4% paraformaldehyde. After dispersing the cells on the slides, they were permeabilized by exposing them to Triton X-100 and incubating for 5 min. The cells were then washed in PBS for 5 min, and the process was repeated three times. To avoid non-specific antibody binding, the cells were blocked with a BSA solution. After washing with PBS 3 times, the cells were exposed to the desired antibody and visualized under a light microscope (Olympus, IX71). Protein and ion content were quantified as indicators of the expression level and ion deposition. To quantify the expression of specific proteins in the IHC technique, the number of cells expressing the specific biomarker in each group was counted using ImageJ software and then normalized to the corresponding total number of cells.

2.6 Statistical Analysis

All experiments were conducted at least in triplicate, and the resultant parameters were expressed as mean \pm standard deviation (SD). Each treated test group was compared to the control group for significant differences using a *t*-test. In addition, we used the one-way ANOVA analysis to analyze the differences between treated samples, considering *p*-values < 0.05 , as statistically significant.

3 Results and Discussion

3.1 Nanovibration-Enhanced Osteogenic Protein Expression

Formation of mineralized nodules is a hallmark of osteogenic differentiation, which can be assessed by monitoring the accumulation of secreted calcium adjacent to mesenchymal stem cells after exposure to a specific stimulus (Fig. 3A). Alizarin red staining showed a significant increase in calcium deposition compared to the control group, which supports the

induction of osteogenic differentiation of HUC-MSCs after 21-day exposing 1-kHz continuous nanovibration.

Commonly, during bone formation, mature osteoblasts produce osteocalcin and osteopontin to regulate bone mineralization. Hence, evaluation of both osteocalcin and osteopontin expression levels provides verification of osteogenic differentiation. Figure 3B shows a remarkable elevation in the levels of osteocalcin and osteopontin expression compared to the control group. Both proteins were expressed at their highest levels in the stimulated groups compared to the control group (Fig. 3B). Furthermore, a significant increase in the expression of collagen type I, which is representative of osteoblast activity, reinforces the induction of osteogenic differentiation. These results are in agreement with previous reports on the capability of nanoscale vibration to induce the osteogenic lineage [11, 18].

3.2 Actin Fiber Rearrangements After Nanovibration Exposure

Actin filaments play a significant role in various biophysical behaviors, such as migration potential and cell motility, as well

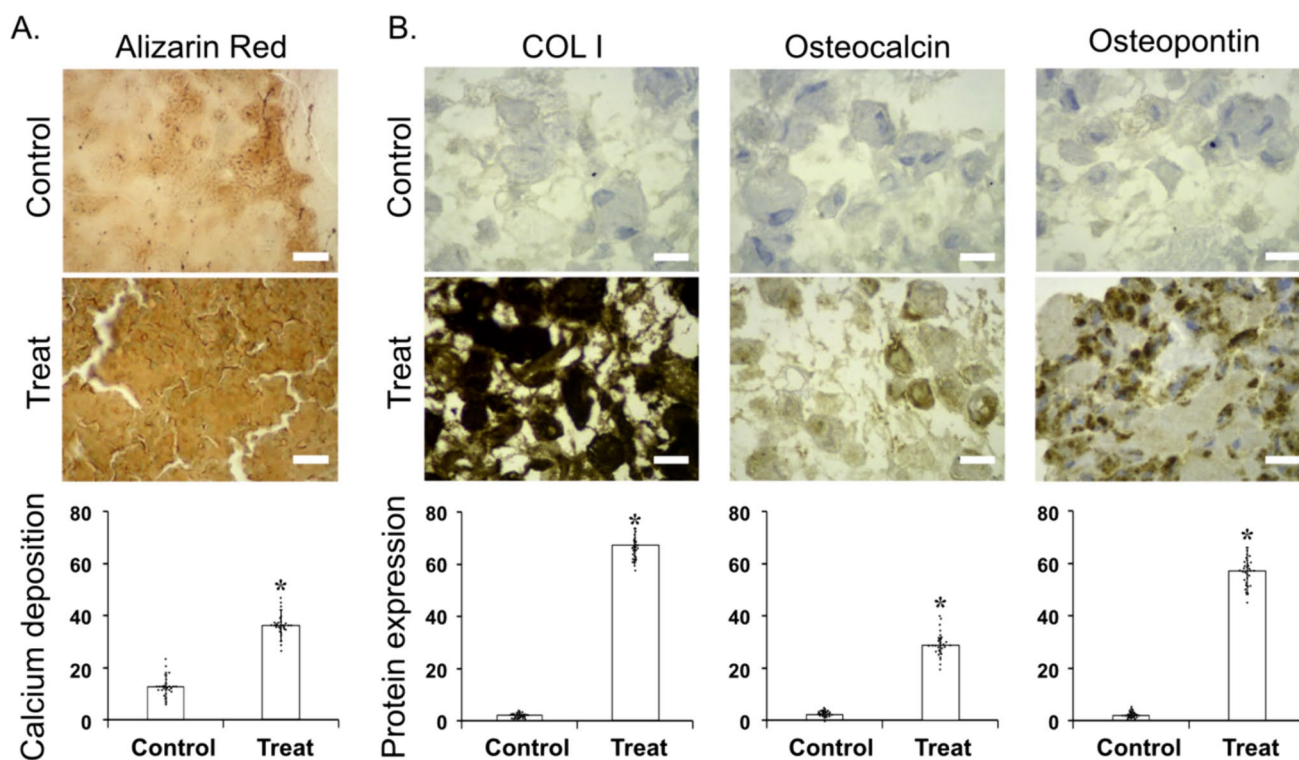


Fig. 3 Representative images of histological and immunohistochemical analyses **A** Alizarin Red staining of HUC-MSCs to quantitatively assess mineralization in control and treated groups. **B** Alterations in

the expression levels of collagen type 1, osteocalcin, and osteopontin in HUC-MSCs before and after 21-day nanovibrational stimuli

as in cell integrity, along with microtubules and intermediate filaments. Therefore, any alteration in the content and arrangement of actin filaments significantly modifies cellular behavior. Here, we examined the alteration in actin filaments under the influence of nanovibration loading for 7, 14, and 21 days.

The first observation from Fig. 4A indicates an increase in nucleus size (Fig. 4B) and number of cell projections, accompanied by an elevation in cell spreading, and it is expected that cells become larger in area during the later stage of differentiation. In addition, the increase in the number of projections may signify involvement in extracellular matrix remodeling, as well as interactions with neighboring cells. These observations resemble evidence associated with osteogenic differentiation [27, 28].

Upon further analysis of the actin structure, it was observed that not only did the average number of actin filaments increase, but they also became thicker after exposure to the nanovibration stimuli (Fig. 4C–E). In addition, prolonged exposure to 1-kHz nanovibration resulted in more aligned and denser arrangements of actin filaments. As previously mentioned, the development of actin filaments plays a remarkable role in several osteogenic-specific cellular processes such as bone ECM remodeling [27, 28].

Figure 4 indicates that additional exposure to nanovibration loading had a more pronounced effect on the actin filaments. In other words, with increasing exposure time, the actin filaments became thicker and more aligned, suggesting that nanovibration significantly influences actin filament dynamics and organization.

3.3 Alteration in Elastic Modulus of HUC-MSCs in Response to Nanovibration

Given the intricate interplay among various elements of the cytoskeleton, alterations in the cytoskeleton designate cell morphology. Because the cytoskeleton serves as a cellular scaffold, it is expected that any alteration in the cytoskeleton changes the mechanical properties of the cell. To measure the local elastic properties, atomic force microscopy was employed to probe Young's modulus of the regions over the nucleus and cytoplasm.

Figure 5 shows the elastic properties of the nucleus and cytoplasm areas of HUC-MSCs in the control and stimulated groups on days 7, 14, and 21. The values for the nucleus and cytoplasm in the control group were similar, with mean values around 3.68 and 3.45 kPa, respectively. As depicted in Fig. 3, the results revealed that exposure to nanovibration for 7 and 14 days did not lead to remarkable changes in the elastic modulus. However, extended exposure to 1-kHz continuous nanovibration for an additional 7 days led to a significant increase in Young's modulus

of both the nucleus and cytoplasm, with a higher impact on the latter. Such modifications are directly linked to the synthesis and rearrangement of cytoskeleton-related proteins such as actin filaments. In the initial days after commencing stimulation, no significant changes in elastic modulus were observed compared with the control group, which was mostly due to the additional time needed for modifications in the physical structure of the protein. However, with an increase in the time of exposure to nanovibration, on day 21, highly organized cytoskeletal filaments with more aligned and higher amounts of actin fibers were observed (Fig. 4), resulting in increased stiffness of cells. This evidence signifies the osteogenic differentiation of HUC-MSCs from a biomechanical perspective because they exhibit significantly higher elastic properties than mesenchymal stem cells.

3.4 Measurements of Viscoelastic Properties of Treated HUC-MSCs

Similar to the evaluation of elastic properties, the viscoelastic properties of the control and stimulated groups were monitored over 7, 14, and 21 days (Fig. 6). To do so, the stress relaxation behavior of the stimulated cells over the nuclear region was measured using atomic force microscopy (Fig. 6A). The results demonstrated that all samples exhibited rapid force decay at the initial stage, followed by a more prolonged relaxation response. The obtained results of apparent viscosity did not exhibit a consistent trend (Fig. 6B). However, the apparent viscosity of the sample subjected to 21-day nanovibration loading was significantly lower than that of the control group. As shown in Fig. 6C, the measured values of E_1 and E_2 show a significant elevation in the instantaneous elastic modulus along with a notable reduction in the equilibrium modulus and viscosity of cells subjected to the 1-kHz continuous nanovibration with an increasing trend when exposed to the additional stimuli. These findings suggest that nanovibration stimuli induce alterations in cytoskeleton organization, resulting in increased cell stiffness and higher resistance to deformation. The concurrent reduction in both E_2 and apparent viscosity along with an increase in E_1 may indicate a more elastic-dominant response, with a reduced potential to dissipate energy during deformation. As shown in Fig. 4, the content, localization and orientation of the actin filaments changed over time, forming more aligned and organized bundle structures over the exposure time of the nanovibration. Such structures exhibit greater resistance to forces. Therefore, the structure becomes stiffer, and a higher

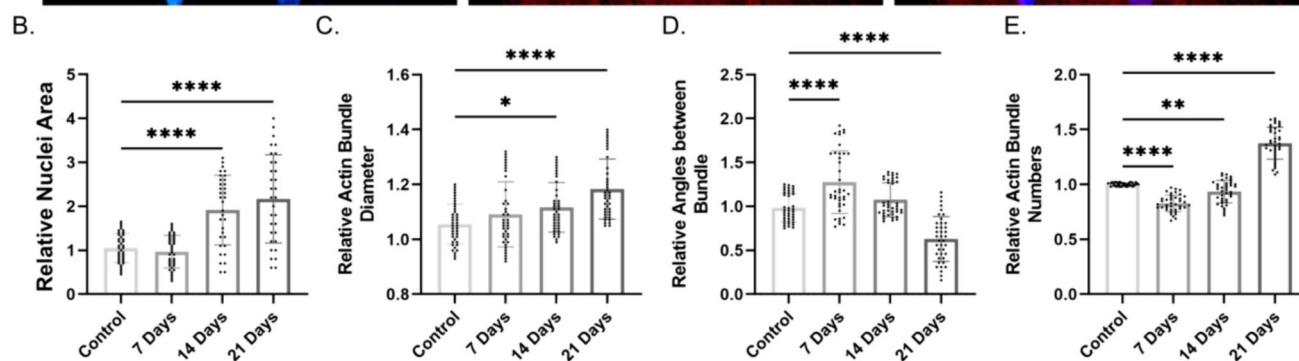
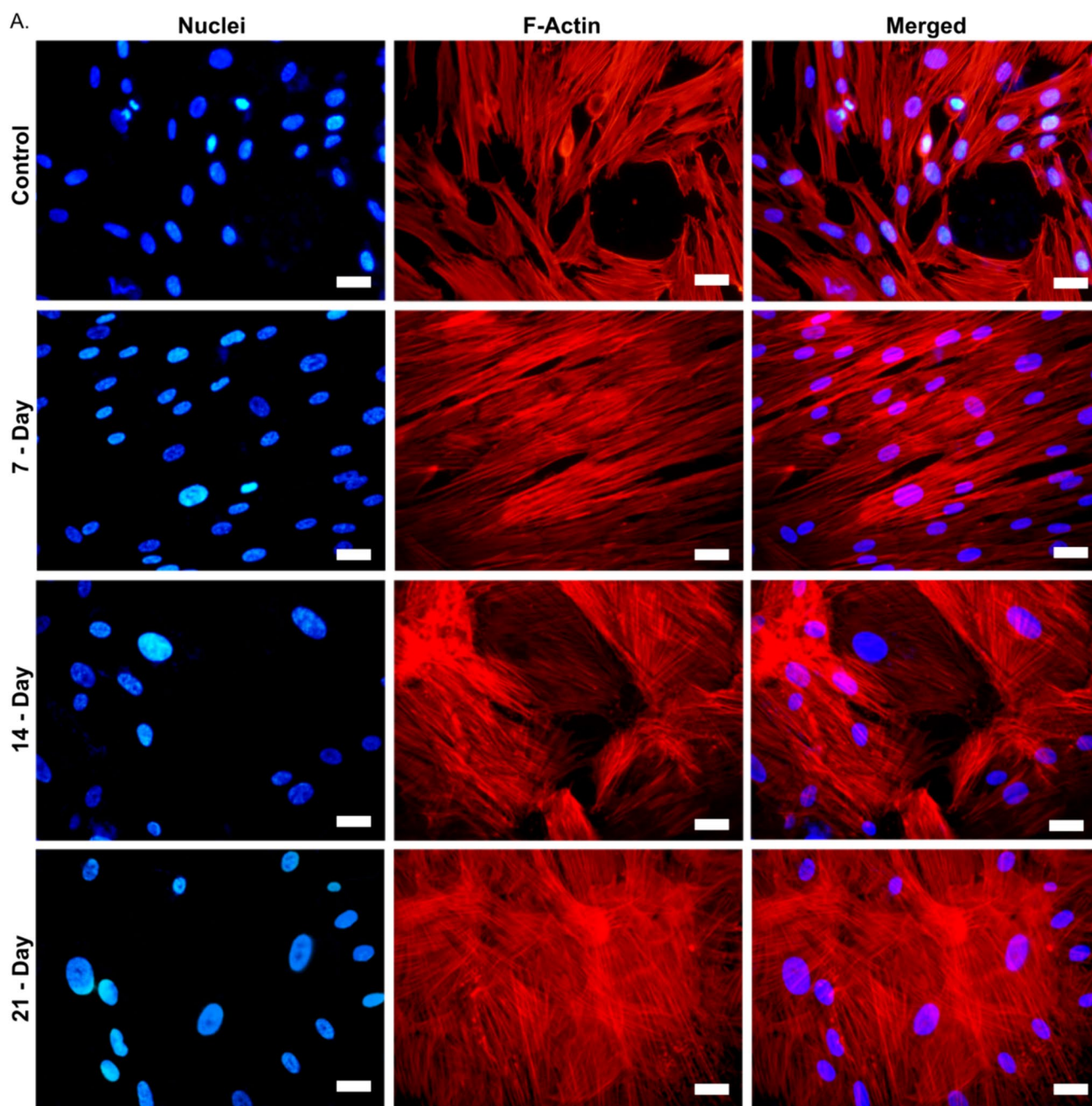


Fig. 4 Representative micrographs of F-actin and nuclei stained in the control and stimulated groups. **B** Elevation in cell nucleus size after exposure to nanovibration stimuli. **C** Alteration in actin bundles arrangement after exposure to nanoscale stimuli for 7, 14, and 21 days. The results demonstrated thicker actin bundles compared to untreated cells. **D** Elevation in the number of actin bundles after nanovibrational stimulation. **E** Exposure to nanovibrational stimuli leads to a more organized network of actin bundles. Scale bar indicates 20 μm . *** p value < 0.0001

magnitude of force is required to indent at the same distance from the cantilever (as shown in Fig. 6A). On the other hand, such a developed structure requires much less time to dissipate the applied force, a behavior observed in 21-day stimulated cells. The initial step in the differentiation process involves the regulation of specific markers at the transcriptional level, and additional time is required for the synthesis and rearrangement of various proteins. During this period, cells undergo a transient state (days 7 and 14), and alterations in higher-level behaviors, such as mechanical properties, are unstable. This interpretation could be the reason for the temporary increase in cell viscosity observed on day 14.

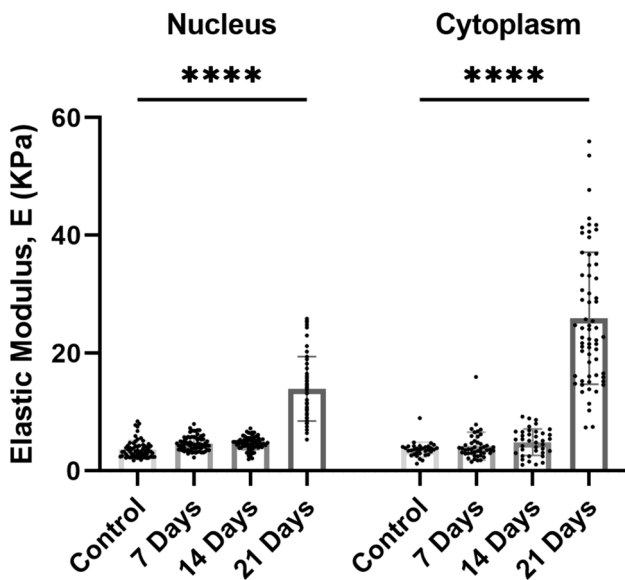


Fig. 5 Alteration in elastic modulus of cytoplasm and nuclear of HUC-MSCs after exposure to 1 kHz continuous nanovibrational loading for 7, 14, and 21 days. *** p value < 0.0001

Overall, it has been well stated that sinusoidal nanokicking (with 1 kHz frequency) is capable of solely promoting osteogenic differentiation in MSCs through upregulation of chemical cascades that contribute to skeletal and muscular system development and function as well as ROCK/RhoA pathways. Application of high frequency, low amplitude loading can stimulate the mechanosensitive receptors which are capable of promoting the release of cytokines that regulate cell behavior, including osteogenic induction among MSCs. Those chemical cascades influence cytoskeleton organization and increase intracellular tension [11, 18]. The nanovibration as an external cyclic loading can also be transferred directly through the cell body as a physical stimulus by cytoskeletal fibrous structure and synergistically contribute to behavioral remodeling of cells through chemical cascades. The cell response is accompanied by cytoskeletal remodeling through actin rearrangement (Fig. 4) which in turn further influences the transmission of force across the cell body as well as the release of cytokines. Such synergy intensifies the regulation of the cell fate as described by the expression of osteogenic markers (Fig. 3).

4 Conclusion

In summary, continuous long-term nanovibrational stimuli with a frequency of 1000 Hz and amplitude of 30–80 nm lead to osteogenic differentiation of HUC-MSCs by enhancing the expression levels of osteocalcin, osteopontin, and collagen type I proteins. Moreover, prolonged exposure to nanovibrational stimuli yielded remarkable effects on actin filament organization and mechanical properties of the cells. However, 7-day and 14-day exposures to nanovibration exhibited negligible effects on the elastic properties of the cells in both the cytoplasm and nucleus areas, indicating the importance of exposure time. After 21-day exposure to nanoscale vibration, stimulated cells showed significantly higher elastic modulus and lower fluidic-like behavior associated with a thicker, denser, and well-organized arrangement in actin fibers, which indicates a tendency towards osteoblast characteristics. The finding of this study would be helpful in the cell-based therapy and tissue engineering applications, when the stem cells required to be treated in vitro and then transplanted.

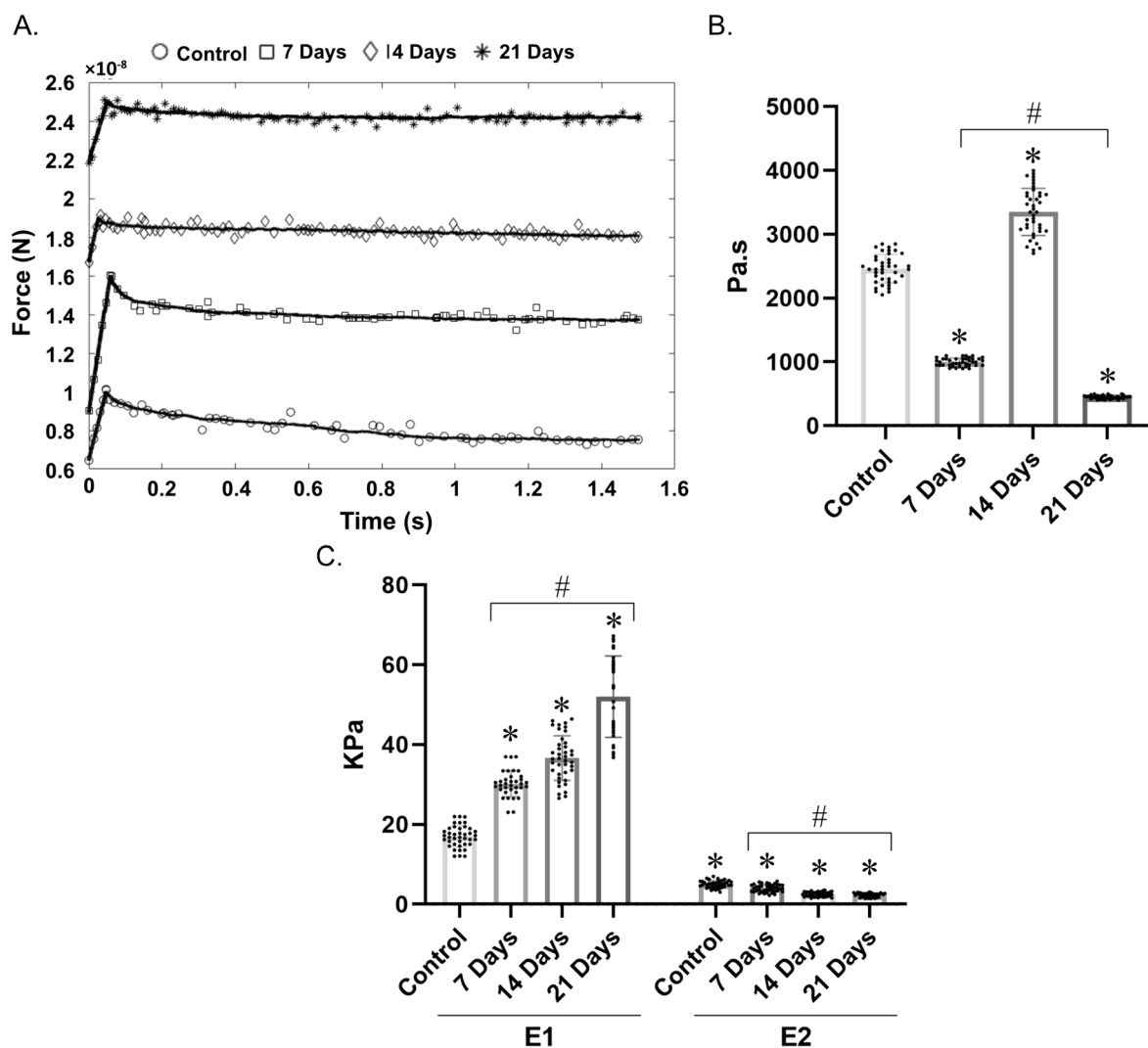


Fig. 6 Viscoelastic behavior of HUC-MSCs before and after exposure to nanovibrational stimuli for different days **A** Force–time curve of control and treated groups. **B** Quantitative results of apparent viscosity. **C** The estimated values of E_1 and E_2

Author Contribution We confirm that all authors, submitting this manuscript, were fully involved in the study and preparation of the manuscript and have neither been employed by a government agency nor as an official representative or on behalf of the government. All authors have given approval to the final version of the manuscript. RRS conducted the experiments and wrote the original and initial drafts. KH, MT-Sh, and AA participated in the technical support and data screening. MT contributed in cell-staining experiment and analysis, and M-MKh, as a project administration, designed the study and methodology, and reviewed the original manuscript.

Funding This study was supported by the Shahid Beheshti University of Medical Sciences (grant no. 30052).

Data Availability The data that support the findings of this study are available from the corresponding author upon reasonable request.

Declarations

Competing Interests The authors declare no competing interests.

Conflict of Interest The authors declare that they have no known competing financial interests or personal relationships that could have appeared to influence the work reported in this paper.

Research Involving Humans and Animals Statement All the experiments were performed in compliance with the approved protocols by the Shahid Beheshti University of Medical Sciences Ethics Committee (Ethical approval number IR.SBMU.REC.1400.032).

References

- West-Livingston, L. N., Park, J., Lee, S. J., Atala, A., & Yoo, J. J. (2020). The role of the microenvironment in controlling the fate of bioprinted stem cells. *Chemical Reviews*, *120*(19), 11056–11092.
- Guilak, F., Cohen, D. M., Estes, B. T., Gimble, J. M., Liedtke, W., & Chen, C. S. (2009). Control of stem cell fate by physical interactions with the extracellular matrix. *Cell Stem Cell*, *5*(1), 17–26.
- Nair, A., Chauhan, P., Saha, B., & Kubatzky, K. F. (2019). Conceptual evolution of cell signaling. *International Journal of Molecular Sciences*, *20*(13), 3292.
- Zhao, J., Griffin, M., Cai, J., Li, S., Bulter, P. E., & Kalaskar, D. M. (2016). Bioreactors for tissue engineering: An update. *Biochemical Engineering Journal*, *109*, 268–281.
- Castro, N., Ribeiro, S., Fernandes, M., et al. (2020). Physically active bioreactors for tissue engineering applications. *Advanced Biosystems*, *4*(10), 2000125.
- Liedert, A., Kaspar, D., Augat, P., Ignatius, A., & Claes, L. (2005). *Mechanobiology of bone tissue and bone cells*. Mechanosensitivity in cells and tissues.
- Liu, P., Tu, J., Wang, W., et al. (2022). Effects of mechanical stress stimulation on function and expression mechanism of osteoblasts. *Frontiers in Bioengineering and Biotechnology*, *10*, 830722.
- Shi, Y., Fu, Y., Tong, W., et al. (2012). Uniaxial mechanical tension promoted osteogenic differentiation of rat tendon-derived stem cells (rTDSCs) via the Wnt5a-RhoA pathway. *Journal of Cellular Biochemistry*, *113*(10), 3133–3142.
- Cheema, U., Chuo, C. B., Sarathchandra, P., Nazhat, S. N., & Brown, R. A. (2007). Engineering functional collagen scaffolds: Cyclical loading increases material strength and fibril aggregation. *Advanced Functional Materials*, *17*(14), 2426–2431.
- Yim, E. K., Darling, E. M., Kulangara, K., Guilak, F., & Leong, K. W. (2010). Nanotopography-induced changes in focal adhesions, cytoskeletal organization, and mechanical properties of human mesenchymal stem cells. *Biomaterials*, *31*(6), 1299–1306.
- Tsimbouri, P. M., Childs, P. G., Pemberton, G. D., et al. (2017). Stimulation of 3D osteogenesis by mesenchymal stem cells using a nanovibrational bioreactor. *Nature Biomedical Engineering*, *1*(9), 758–770.
- Yim, E. K., Pang, S. W., & Leong, K. W. (2007). Synthetic nanostructures inducing differentiation of human mesenchymal stem cells into neuronal lineage. *Experimental Cell Research*, *313*(9), 1820–1829.
- Nikukar, H., Childs, P. G., Curtis, A. S., et al. (2016). Production of nanoscale vibration for stimulation of human mesenchymal stem cells. *Journal of Biomedical Nanotechnology*, *12*(7), 1478–1488.
- Hou, W., Zhang, D., Feng, X., & Zhou, Y. (2020). Low magnitude high frequency vibration promotes chondrogenic differentiation of bone marrow stem cells with involvement of β -catenin signaling pathway. *Archives of Oral Biology*, *118*, 104860.
- Karimi, E., Vahedi, N., Sarbandi, R. R., et al. (2023). Nanoscale vibration could promote tenogenic differentiation of umbilical cord mesenchymal stem cells. *In Vitro Cellular & Developmental Biology-Animal*, *59*(6), 401–409.
- Zhang, C., Lu, Y., Zhang, L., et al. (2015). Influence of different intensities of vibration on proliferation and differentiation of human periodontal ligament stem cells. *Archives of Medical Science*, *11*(3), 638–646.
- Fletcher, D. A., & Mullins, R. D. (2010). Cell mechanics and the cytoskeleton. *Nature*, *463*(7280), 485–492.
- Nikukar, H., Reid, S., Tsimbouri, P. M., Riehle, M. O., Curtis, A. S., & Dalby, M. J. (2013). Osteogenesis of mesenchymal stem cells by nanoscale mechanotransduction. *ACS Nano*, *7*(3), 2758–2767.
- Khani, M.-M., Tafazzoli-Shadpour, M., Goli-Malekabadi, Z., & Haghhighipour, N. (2015). Mechanical characterization of human mesenchymal stem cells subjected to cyclic uniaxial strain and TGF- β 1. *Journal of the Mechanical Behavior of Biomedical Materials*, *43*, 18–25.
- Khani, M.-M., Tafazzoli-Shadpour, M., Rostami, M., Peirovi, H., & Janmaleki, M. (2014). Evaluation of mechanical properties of human mesenchymal stem cells during differentiation to smooth muscle cells. *Annals of biomedical engineering*, *42*, 1373–1380.
- Titushkin, I., & Cho, M. (2007). Modulation of cellular mechanics during osteogenic differentiation of human mesenchymal stem cells. *Biophysical Journal*, *93*(10), 3693–3702.
- Dimitriadis, E. K., Horkay, F., Maresca, J., Kachar, B., & Chadwick, R. S. (2002). Determination of elastic moduli of thin layers of soft material using the atomic force microscope. *Biophysical Journal*, *82*(5), 2798–2810.
- Pelleg, J. (2013). *Mechanical properties of materials* (Vol. 190, pp. 1–84). Springer.
- Moreno-Flores, S., Benitez, R., Dm Vivanco, M., & Toca-Herrera, J. L. (2010). Stress relaxation and creep on living cells with the atomic force microscope: A means to calculate elastic moduli and viscosities of cell components. *Nanotechnology*, *21*(44), 44510.
- Darling, E., Zauscher, S., & Guilak, F. (2006). Viscoelastic properties of zonal articular chondrocytes measured by atomic force microscopy. *Osteoarthritis and Cartilage*, *14*(6), 571–579.
- Tabatabaei, M., Tafazzoli-Shadpour, M., & Khani, M. M. (2019). Correlation of the cell mechanical behavior and quantified cytoskeletal parameters in normal and cancerous breast cell lines. *Biorheology*, *56*(4), 207–219.
- Putra, V. D. L., Kilian, K. A., & Knothe Tate, M. L. (2023). Bio-mechanical, biophysical and biochemical modulators of cytoskeletal remodelling and emergent stem cell lineage commitment. *Communications Biology*, *6*(1), 75.
- Khan, A. U., Qu, R., Fan, T., Ouyang, J., & Dai, J. (2020). A glance on the role of actin in osteogenic and adipogenic differentiation of mesenchymal stem cells. *Stem Cell Research & Therapy*, *11*(1), 283.

Publisher's Note Springer Nature remains neutral with regard to jurisdictional claims in published maps and institutional affiliations.

Springer Nature or its licensor (e.g. a society or other partner) holds exclusive rights to this article under a publishing agreement with the author(s) or other rightsholder(s); author self-archiving of the accepted manuscript version of this article is solely governed by the terms of such publishing agreement and applicable law.